**INTERNATIONAL DESIGN CONFERENCE – DESIGN 2022**
https://doi.org/10.1017/pds.2022.38

# Truss Parametrization of Topology Optimization Results with Curve Skeletons and Meta Balls

M. Denk [1], K. Rother [2] and K. Paetzold [3,✉]

[1] Universität der Bundeswehr München, Germany, [2] Munich University of Applied Sciences, Germany,
[3] Technische Universität Dresden, Germany

✉ kristin.paetzold@tu-dresden.de

**Abstract**

Truss-like shapes can occur in topology optimization described by an assembly of finite elements or its boundary represented as a polygon mesh. Such shape description does not cover a common engineering parametrization like the lines of a frame structure and its corresponding cross-section. This article addresses the truss-parametrization of such optimization using curve skeletons and Meta Balls. While the curve skeleton is common in the truss-parametrization, including Meta Balls can lead to an overall implicit and smooth shape description.

*Keywords: topological optimisation, reverse engineering, computer-aided design (CAD)*

## 1. Introduction

Structural optimization such as density-based topology optimization leads to a finite element model as a resulting representation (Bendsoe and Sigmund, 2004). Each element is typically applied with a local density variable, which scales the corresponding stiffness matrix (Bendsøe and Sigmund, 1999). By restricting the amount of possible voluminal, the density should be distributed to minimize the corresponding objective, such as thermal or elasto static compliance.

As a common mesh topology an assembly of squares or cubes is often chosen due to the equal and uniform size, which leads to 2D and 3D image representation. On such representation common algorithms in digital image processing such as morphological or convolutional filters can be applied (Burger and Burge, 2009), which offers the advantages of fast computaionial processing. While such representation is common in image processing, engineering applications requieres a shape parametric to be able to fulifill manufacturing constraints (Adam and Zimmer, 2015) or even apply shape optimization (Bandara et al., 2016; Xia et al., 2020). Topology optimization can lead to smooth results (Christiansen et al., 2015) or even directly to freeform surfaces (Gao et al., 2020), which often does not lead to a suitable parameterization desirable for matching the shape to manufacturing. Particular for selective laser melting the geometry has to statisfy constraints such as minimum local size and avoiding overhang angles (Adam and Zimmer, 2015), that should be adjustable by the selected parametric. Moreover, the topology-optimized design must often be reconstructed for verification (Cuillière et al., 2018). If this verification fails, automatic adjustment is required, especially for optimization results with a large number of branches, as often occurs in thermal topology optimization (Joo et al., 2018).

Converting topology optimization results into such parametrization is one of the recent research challenges, which can be solved by curve (Denk et al., 2021b; Yin et al., 2020) or surface skeletons (Denk et al., 2021c). The original concept of skeletons is derived from Blum's medial skeletons (Blum, 1967). By choosing the locus of the center of so-called maximally inscribed balls, a medial skeleton can be obtained by connecting the centers. The original shape itself can be fully restored by the unification of these balls. Recent skeleton-based reverse engineering approaches choose to extrude primitive cross-sections along these skeleton lines (Cuillière et al., 2018; Nana et al., 2017; Stangl and Wartzack, 2015) or apply free form surface reconstruction (Bremicker et al., 1991; Denk et al., 2021b). Afterward, the shape is assembled using an implicit representation CSG of these cylindrical primitives (Cuillière et al., 2018; Nana et al., 2017) or connecting the control points of the explicit free form surfaces (Bremicker et al., 1991; Denk et al., 2021b). The fundamental concept of these medial balls of the unification of each ball is covered by the unification of cylinders and spheres (Cuillière et al., 2018; Nana et al., 2017) or the selection of reasonable control point positions (Bremicker et al., 1991; Denk et al., 2021b). CSG can lead to an implicit representation with sharp edges, while free form surfaces can leads to a smooth but explicit representation (Bremicker et al., 1991; Denk et al., 2021b). An implicit smooth shape descriptor is desirable due to advances in topology modification or the use of Boolean operations.

As an alternative, this article deals with the selection of so-called meta-balls, which can directly lead to a smooth geometry without post-processing. This article first gives a brief overview of skeleton-based reconstruction in Chapter two, followed by the basics of using Meta Balls in Chapter three. Chapter four focuses on the methods for fully automatic skeleton parameterization using meta-ball, visually guided by a use case. Chapter five applies the presented parameterization to various topology optimization use cases considering thermal and elastostatic compliance. Furthermore, the parametrization of an elastostatic optimization result is visually compared to common CSG and subdivision surface reconstruction methods. Furthermore, a size-constrained use case is presented where the local size can be adjusted directly. Finally, an example of automatic verification of the topology optimization result using fully automatic reconstruction is presented.

## 2. State of the Art

In the recent publications, the beamline of topology optimized shapes can be approximated by a contraction method applied on a polygon mesh (Cuillière et al., 2018; Stangl and Wartzack, 2015), a medial axis transformation (Mayer and Wartzack, 2020), or morphological thinning applied on images (Bremicker et al., 1991; Denk et al., 2021b; Xia et al., 2020; Yin et al., 2020). These skeletonization concepts can be derived from Blum's medial balls (Tagliasacchi et al., 2016) and should lead to similar skeletons. Typically, there are several desirable properties such as homotopy preservation, saleability, or regularization (Sobiecki et al., 2014; Tagliasacchi et al., 2016), which should be taken into account. The topological properties (e.g. homotopy) of the skeleton and the corresponding 3D object are the same if the number of cavities, objects and holes are also the same (Morgenthaler, 1981). Such conditions can be used to construct a homotopy preserving thinning method by using the simple point condition for digital images (Morgenthaler, 1981). A simple point is a point on the surface, which does not change the topological properties during the erosion (Lee et al., 1994; Morgenthaler, 1981). The authors of (Lee et al., 1994) use the Euler characteristic and adjunct tree to find such simple points for the skeletonization. Such thinning algorithm can be directly applied to finite elements such as voxels (Denk et al., 2021b, 2021c; Yin et al., 2020). Additionally also predefined points such as boundary conditions may be taken into account for skeletonization (Xia et al., 2020). Figure 1 shows one example of the skeletonization of a binary image and its segmentation.

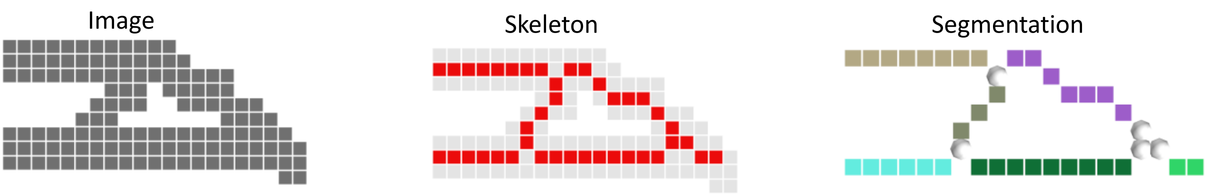


**Figure 1. Binary image skeleton of the image and segmentation of the skeleton.**



https://doi.org/10.1017/pds.2022.38 Published online by Cambridge University Press

The segmentation can be determined by considering the local neighborhood of each voxel. Branch points share more than two connections, while endpoints are only connected to one other voxel. Based on these curve or surface skeletons, various of different shape descriptors may be taken into account. The common shape description is the unification of cylinders along with the curve skeleton and spheres at branches and endpoints leading to CSG (Nana et al., 2017; Yin et al., 2020). As another alternative, the authors of (Stangl and Wartzack, 2015) extrude predefined cross-sections such as circles or ellipses along a fitted curve for the reconstruction. Such representation leads to a highly efficient parametrization with only a few necessary parameters. The unified primitives can be further processed by applying blended surfaces (Yin et al., 2020) to smooth the sharp edges occurring due to the unification.

While the unification of primitives can lead to sharp edges, the authors of (Amroune et al., 2022; Denk et al., 2021b, 2021c, 2021a) applied free-form surfaces. By constructing a control polygon mesh, the geometry can be calculated using the subdivision surfaces (Catmull and Clark, 1978), leading to a smooth shape description. The authors of (Denk et al., 2021b) determined the control mesh by using the distance value of the along the curve-skeleton. A circular cross-section is approximated by using a square cross-section control grid, which is extruded along with the curve skeleton. This leads to a polygon control mesh for each truss element, which is unified to each other considering the convex hull. The authors of (Denk et al., 2021a) extended that approach by using predefined cross-sections, leading to rectangular control point positions. Instead of a control polygon mesh, the authors of (Amroune et al., 2022) use periodic B-splines that are raised along specific ray lines. The individual beams are then connected at junctions by a connector surfaces. An alternative to such CSG or free-form surfaces are Meta Balls, which are discussed in this article. Such Meta Balls implicitly connects to neighbour balls without the additionall effort calculating the intersections.

## 3. Introduction in Soft Objects, Meta Balls, Convolutional Surfaces

For skeletonization, implicit functions can be used for so-known convolutional surfaces (Bloomenthal and Shoemake, 1991; Hubert and Cani, 2012), which can be used for shape modeling (Alexe et al., 2007; Karpenko et al., 2002). Based on a geometry function consisting of points edges or polygons, the skeleton is hulled with a kernel like the a gaussian function (Blinn, 1982), the square inverse distance function, or polynomial functions (Hitoshi et al., 1985; Wyvill et al., 1986). Meta balls (Hitoshi et al., 1985) or soft objects (Wyvill et al., 1986) uses one common kernel functions particular in designing organic shapes (Blinn, 1982; Bloomenthal and Wyvill, 1997; Pan et al., 2016; Xu and Wu, 2016). Figure 2 shows the interaction of Meta Balls in Blender. By defining spherical objects with a certain influence zone, two balls can be connected by pushing the balls to each other. By assembling various of these balls, complex shapes such as the T-Junction can be designed.

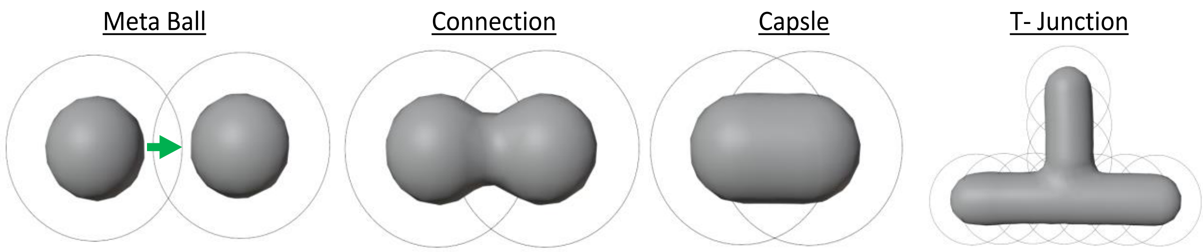


**Figure 2. Meta balls in Blender. If the influence region of two Meta Balls touches, these balls will be connected directly depending on the chosen fall-off curve.**

Meta balls use a so-called fall-off curve based on distance metrics, in the influence region for the connection of the balls to each other. Meta balls use a special kind of that kernel function with

$$f_i(r_i) = \begin{cases} 1 - 3\left(\frac{r_i}{R}\right)^2; & 0 \le r_i \le R\frac{1}{3} \\ \frac{3}{2}\left(1 - \left(\frac{r_i}{R}\right)\right)^2; & R\frac{1}{3} < r_i \le R \\ 0; & r_i > R \end{cases} . \quad (1)$$



https://doi.org/10.1017/pds.2022.38 Published online by Cambridge University Press

(Hitoshi et al., 1985). As alternative the authors of (Blinn, 1982) suggested as a distance function

$$f_i(r_i) = T\, e^{\frac{B_i}{R_i^2} r_i^2 - B_i} \tag{2}$$

where $T$ can be chosen as a canonical value like 1 and the blobbiness parameter $B_i$ can be changed by arbitrary variation of the shape connection. While the meta ball equation can be computed locally, the gaussian function is defined over the entire domain, resulting in higher computational costs. To determine the geometry each contribution (ball) has to be added to a global function $F$

$$F(x) = \sum_i^n f_i(||\boldsymbol{x} - \boldsymbol{x}_i||) \tag{3}$$

on which the contour of the Meta Balls can be defined as a level set function calculating the isolines with

$$F(x) - L = 0 \tag{4}$$

on which $L$ is an arbitrary scalar value restricting a threshold (Blinn, 1982). Figure 3 illustrates the level set function and the resulting shape abstracted from this geometry on different circles with the same radius.

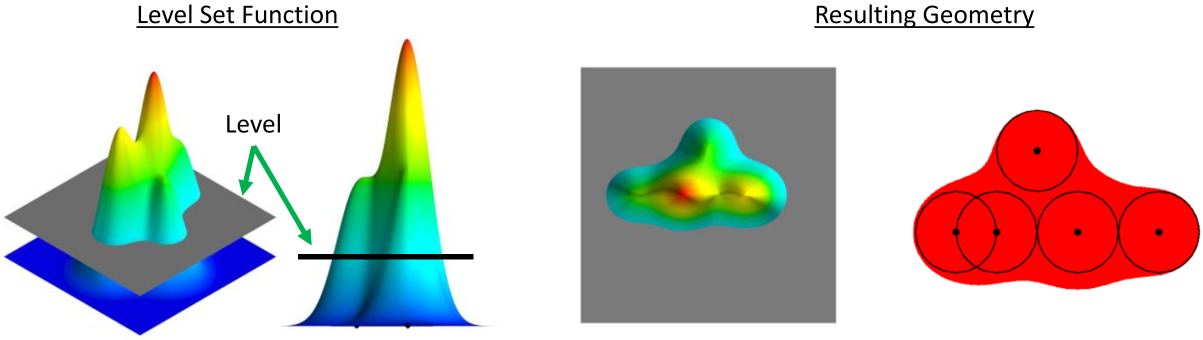


**Figure 3. Soft objects with $B_i$ = -0.75 using the distance function of (Blinn, 1982).**

The resulting geometry shows that if all circles are smoothly connected to each other. This geometry can now be adjusted by the variation of the "blobbiness" by changing $B_i$. Meta Balls themselves can lead to unexpected behavior so that shapes that are not overlapping are connected, and additionally, blobs can occur in unexpected areas (Angles et al., 2017). By embedding additional user interaction in the form of 2D sketches, the Meta Balls can be guided to the desired shape description (Angles et al., 2017). The following section deals with the fully automated reconstruction of topology optimization results using the curve skeleton and the Meta Balls proposed in Blender 2.93.

## 4. Meta Ball and Curve Skeleton supported Surface Reconstruction

If a topology optmization is applied directly on a 3D image representation (voxels), the result can directly be used for the following methods. For other results (e.g. polygon meshes, polyhedral) a rasterization is first requiered, so that the curve skeletonization with thinning (Lee et al., 1994) can directly be considered. Based on the binary skeleton, a segmentation algorithm is performed, leading to individual beam lines. These beam lines are simplified using a colapse metric prupused in the following. Based on thse polyline the local raidus of the optimizatio nresult is estimated by the Euclidian distance transformation. Finannly meta balls can placed along the polyline with the corresponding radius. The nesscarry steps are visualized in the Figure 4 for use-case.



https://doi.org/10.1017/pds.2022.38 Published online by Cambridge University Press

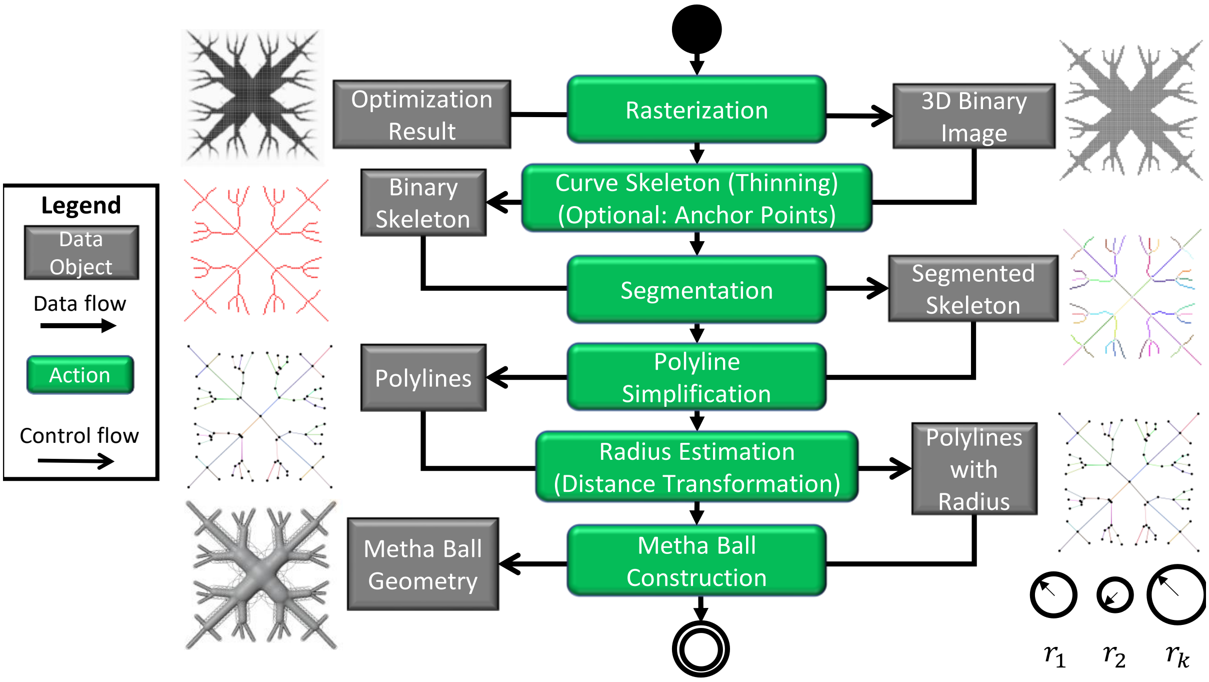


**Figure 4. Skeleton supported shape reconstruction with meta balls**

The curve skeletons represented as binary images can be segmented into individual branches using the connectivity of each skeletal point. To reduce the number of lines based on the segmented skeleton, a collapsing metric is chosen, which ensures that a point $\boldsymbol{v}_i^k$ and the following point $\boldsymbol{v}_i^{t+k}$ along the polyline, $i$ is in a certain quadratic distance $\epsilon$ with

$$\left\|\boldsymbol{v}_i^{t+k} - \boldsymbol{v}_i^k\right\| \leq \epsilon. \tag{6}$$

The selection of the point order can be chosen by different criteria, such as starting from the first point $\boldsymbol{v}_i^0$ of the voxel chain and proceeding until the polyline with $\boldsymbol{v}_i^t$ violate the distance condition.
As restrictions for $\epsilon$ the properties of the digital image and the provided thinning method can be considered. Due to the thinning algorithm, it is ensured that the local neighborhood for skeletal points consists only of points located at the voxel chain so that another voxel chain has to be at least two voxels distance. Therefore, to avoid the intersection of the collapsed polylines to another, the maximum distance $d$ between the original voxel line and the polyline should not exceed 1.5. Figure 5 shows the impact of the collapse metric for different distance metrics. By increasing $\epsilon$ the resulting polylines are reduced by additionally preserving the topological properties.

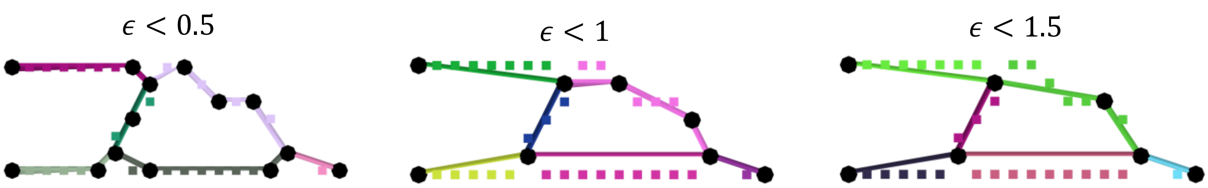


**Figure 5. Simplification of the curve skeleton. By increasing the metric the collapsed skeleton can be simplified. The maximum simplification can be achieved by its topological configuration.**

For the reconstruction with Meta Ball the implementation in Blender 2.93 is chosen, on which a specific radius $r$ and its corresponding stiffness factor $s$ can be applied for each ball. Due to the implicit behavior of Meta Balls, finding an accurate radius can be challenging. Figure 6 shows the result of using Meta Balls along the polyline with circular cross-sections



https://doi.org/10.1017/pds.2022.38 Published online by Cambridge University Press

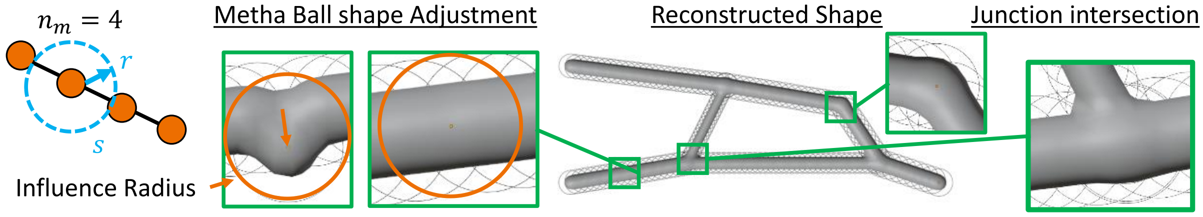


**Figure 6. Meta ball reconstruction $s = 2$. Along the polyline, several balls are placed, which are automatically connected to each other.**

The overall shape shows a smooth surface and organic-like surface representation. These balls can now be adjusted by changing the position or the radius. As an approximation the number of segments can be approximated with

$$n_m = round\left(\frac{w}{r}\,||\boldsymbol{v}_{i+1} - \boldsymbol{v}_i||\right) \tag{7}$$

leading to overlapping Meta Balls and influence radiuses. The following figure shows the variation of the number of Meta Balls along each poly segment increasing $w$.

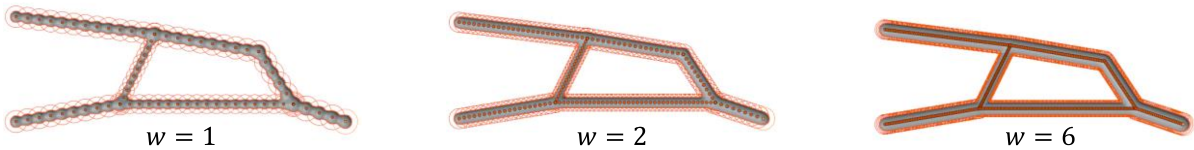


**Figure 7. Variation of the resolution of Meta Balls along the polylines. By increasing the number of the Meta Balls along one segment, the continuity of the local cross-section size can be changed.**

If a too small number of Meta Balls are chosen, the surface leads to a smooth but high steady changing shape. A factor of $w = 6$ leads to a huge amount of Meta Balls without improving the reconstructed geometry. The reconstruction with Meta Balls is quite flexible, and due to its connection properties, a smooth surface is always presented. Calculating points of the surface can be challenging due to its implicit representation. In the following section, the Meta Ball representation is compared to other shape descriptors.

## 5. Case Studie Results and Discussion

In the following case studies, different shape descriptors for surface reconstruction are first presented. Then, various use cases of thermal compliance optimization are considered, followed by automatic adjustment of the Meta Ball radius to satisfy local size constraints. Third, the reconstructed Meta Ball is verified using finite element analysis considering deformations. This Meta Ball shape descriptor can be compared to image representation, polygon mesh, subdivision surfaces (Catmull-Clark) and CSG consisting of spheres and cylinders. Figure 8 shows the different shape descriptors derived from a static 3D elasto-compliance optimization.

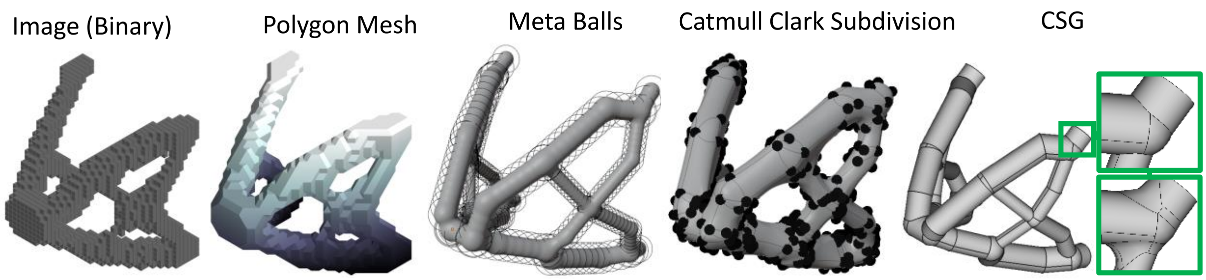


**Figure 8. Comparison of the different Shape descriptors minimizing elasto static compliance**



https://doi.org/10.1017/pds.2022.38 Published online by Cambridge University Press

While the image, polygon mesh and CSG result in an unsmoothed surface, Meta Balls and Catmull-Clark subdivision surfaces tend to give an overall smooth surface description. Moreover, the reconstructed size differs from each other depending on the parameterization chosen. While Meta Balls and CSG tend to provide a more accurate shape coverage of the image, subdivision surface overestimate the optimization result. Constructive solid geometry and subdivision surfaces require joining objects such as spheres (Yin et al., 2020) or convex hulls (Denk et al., 2021a), as opposed to automatically joining Meta Balls. The main drawback of the presented Meta Ball is the selection of an appropriate level for the level set function. While constructive solid geometry and subdivision surfaces can directly represent the explicit surface, the implicit level function estimates the surface, e.g., by considering isocontour surfaces. Similarly, subdivision surfaces and constructive solid geometry are widely used shape descriptions, while Meta Balls are rarely used in commercial software packages and industrial engineering applications. Such descriptions always lead to organic looking objects due to the kernel function and are therefore limited to use cases like the design of organs in medical technology (Pan et al., 2016) or topology optimization results.

The presented parameterization can be applied to the optimization results of thermal or fluid mechanical topology optimization presented (Dede, 2009; Denk et al., 2021d). In particular, considering the minimization of thermal compliance can lead to more complex design proposals than the minimization of elastostatic compliance (Denk et al., 2020). Figure 9 shows such minimization of thermal compliance with (Denk et al., 2021d) for different use-caes and furthermore their skeletonization, segmentaiton and polyline simplification.

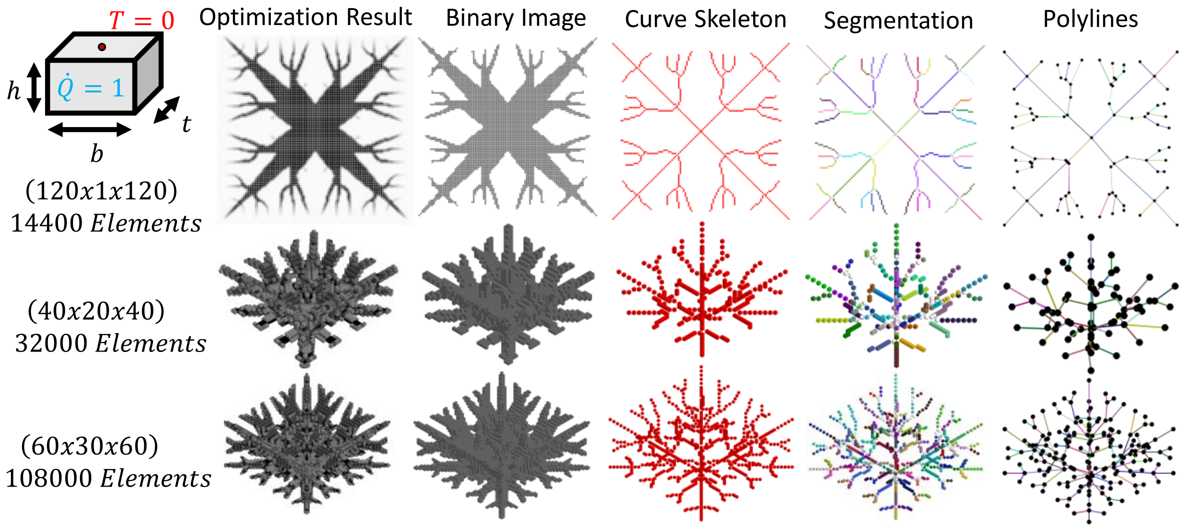


**Figure 9. Case study: skeletonization of use cases minimizing thermal compliance**

Compared to the usecase of elasto static compliance minimization, the results of Figure 10 leads to more branched results. The skeletonization and polyline simplification leads to a reasonable curve approximation of the beam line for all three cases. The manual reconstruction of such beamlines can be very time consuming and error prone, because the huge amount of beam lines are often oriented differently. The main dissatvantage of this curve skeletonization is that each shape is treated as an object that can be constructed by extruding a circular cross section. However, in topology optimization, solid or planar geometries can also be occur, which are poorly covered by the curve skeleton.

One of the major adavances is the still existing shape parametirzation of all of these shape descriptors. Such parametirzation can be used to fuilifill manufacturing constraints such statisfying minimium size control for selective laser melting or reducing overhang angles changing the skeleton coordinates. Figure 10 shows the meta ball reconstruction of the 3D use cases visualized in Figure 10. Additionally, the corresponding radii of the meta balls are scaled up to the minimum allowable size.



https://doi.org/10.1017/pds.2022.38 Published online by Cambridge University Press

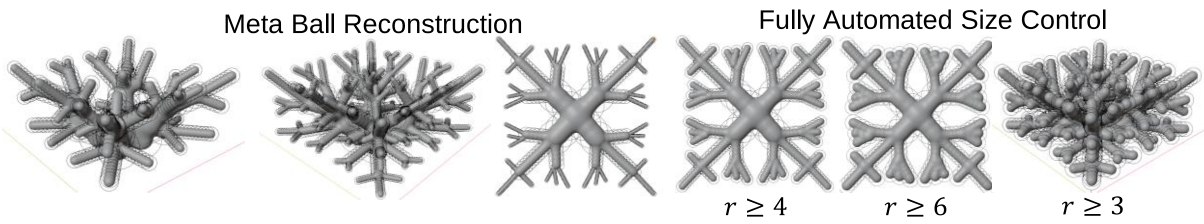


**Figure 10. Meta Ball parametrization for automatic size control**

Such fully automatic size control is desirable for additive manufacturing, especially with such a large number of branches. In addition, the curve skeleton can be adjusted so that the corresponding shape requires a smaller support structure by reducing the overhang angle. While controlling the size is a relatively simple task when such parameterization is available, reducing the overhang angle is a challenge and should be futher discussed in future works. In addition, a change in geometry may affect the corresponding objective, which requires therfore verification of the reconstructed result.
Once a suitable Meta Ball surface has been determined, the reconstruction of the topology optimization result can now be verified considering the maximum displacement using the corresponding geometry and, if necessary, the adapted geometry fulifilling manufacturing specifications. Figure 11 shows the use-case for the compliance topology optimization using solid isotropic mateiral penaltriaztion with a penalty exponent $p = 3$ for a given volumia ratio $\Omega/\Omega_0$.

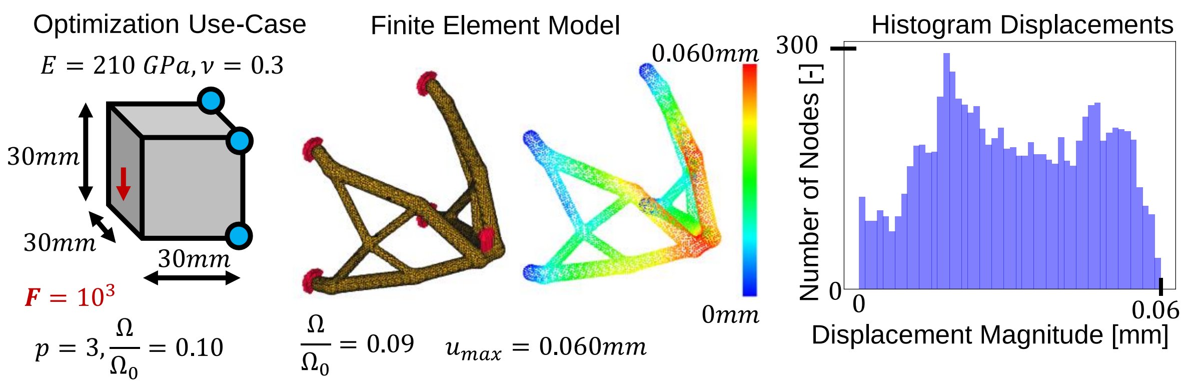


**Figure 11. Verification sample in terms of maximum displacement and volumina ratio of the topology optimzation use-case. (Cyan: fixed constraints)**

The volume ratio differs from the selected topology optimization result to the reconstructed Meta Ball object by 0.01, which is negligible. While this use case uses a manual setup of the finite element model, future work can automatically account for the boundary and load conditions. This offers the possibility of sequential topology optimization followed by verification, or size and shape optimization using these Meta Balls. If the displacement does not meet the given specification, the size of the radii of the Meta Balls can be automatically adjusted until the specification is met.

## 6. Summary

This article describes the use of so-called metaballs and curve skeletons for reconstruction in topology optimization. The main goal is to obtain a beam parametric that can be used to verify or adjust the optimization result. To achieve a compact beam description, skeletonization by thinning is first performed. To simplify the individual skeleton curves, a simplification via a collapse metric is introduced. The individual skeleton curves are simplified until a certain distance to the skeleton points is exceeded. Based on this simplified skeleton, Meta Balls be applied. These Meta Balls are placed along the curve skeleton by a certain distance, with each sphere seamlessly following the others. This parametriaztion is applied to certain use-cases.First, these Meta Balls are visually compared to common surface descriptions, from which their main topological advantages emerge. Meta Balls offer the advantage that they automatically connect seamlessly to neighboring Meta Balls without the need to



https://doi.org/10.1017/pds.2022.38 Published online by Cambridge University Press

specifically consider these cases. Secound based on the available parameters, local size constraints were directly ensured for a heat sink use case. Third, a topology optimization result was reconstructed using Meta Balls for automated verification.
In summary, by using a curve skeleton in combination with Meta Balls, an automated parameterization can be achieved, which in particular allows the automatic connection of beams in an automated way. Such an automation is desirable in the software implementations, because in contrast to CSG and subdivision surfaces no special cases and extra solutions are necessary. The biggest disadvantage compared to the other form descriptions is the restriction to the kernel function, so that often only organic objects can be considered meaningfully.

## References


Adam, G.A.O., Zimmer, D., 2015. On design for additive manufacturing: evaluating geometrical limitations. Rapid Prototyp. J. 21, 662–670. https://doi.org/10.1108/RPJ-06-2013-0060

Alexe, A., Barthe, L., Cani, M.P., Gaildrat, V., 2007. Shape Modeling by Sketching Using Convolution Surfaces, in: ACM SIGGRAPH 2007 Courses, SIGGRAPH '07. Association for Computing Machinery, New York, NY, USA, pp. 39-es. https://doi.org/10.1145/1281500.1281550

Amroune, A., Cuillière, J.-C., François, V., 2022. Automated Lofting-Based Reconstruction of CAD Models from 3D Topology Optimization Results. Comput.-Aided Des. 145, 103183. https://doi.org/10.1016/j.cad.2021.103183

Angles, B., Tarini, M., Wyvill, B., Barthe, L., Tagliasacchi, A., 2017. Sketch-Based Implicit Blending. ACM Trans Graph 36. https://doi.org/10.1145/3130800.3130825

Bandara, K., Rüberg, T., Cirak, F., 2016. Shape optimisation with multiresolution subdivision surfaces and immersed finite elements. Comput. Methods Appl. Mech. Eng. 300, 510–539. https://doi.org/10.1016/j.cma.2015.11.015

Bendsoe, M.P., Sigmund, O., 2004. Topology Optimization: Theory, Methods, and Applications, 2nd ed. Springer-Verlag, Berlin Heidelberg. https://doi.org/10.1007/978-3-662-05086-6

Bendsøe, M.P., Sigmund, O., 1999. Material interpolation schemes in topology optimization. Arch. Appl. Mech. 69, 635–654. https://doi.org/10.1007/s004190050248

Blinn, J.F., 1982. A Generalization of Algebraic Surface Drawing. ACM Trans. Graph. 1, 235–256. https://doi.org/10.1145/357306.357310

Bloomenthal, J., Shoemake, K., 1991. Convolution Surfaces, in: Proceedings of the 18th Annual Conference on Computer Graphics and Interactive Techniques, SIGGRAPH '91. Association for Computing Machinery, New York, NY, USA, pp. 251–256. https://doi.org/10.1145/122718.122757

Bloomenthal, J., Wyvill, B., 1997. Introduction to Implicit Surfaces. Morgan Kaufmann Publishers Inc., San Francisco, CA, USA.

Blum, H., 1967. A Transformation for Extracting New Descriptors of Shape, in: Wathen-Dunn, W. (Ed.), Models for the Perception of Speech and Visual Form. MIT Press, Cambridge, pp. 362–380.

Bremicker, M., Chirehdast, M., Kikuchi, N., Papalambros, P.Y., 1991. Integrated Topology and Shape Optimization in Structural Design∗. Mech. Struct. Mach. 19, 551–587. https://doi.org/10.1080/08905459108905156

Burger, W., Burge, M.J., 2009. Principles of Digital Image Processing, Undergraduate Topics in Computer Science. Springer London, London. https://doi.org/10.1007/978-1-84800-191-6

Catmull, E., Clark, J., 1978. Recursively generated B-spline surfaces on arbitrary topological meshes. Comput.-Aided Des. 10, 350–355. https://doi.org/10.1016/0010-4485(78)90110-0

Christiansen, A.N., Bærentzen, J.A., Nobel-Jørgensen, M., Aage, N., Sigmund, O., 2015. Combined shape and topology optimization of 3D structures. Comput. Graph., Shape Modeling International 2014 46, 25–35. https://doi.org/10.1016/j.cag.2014.09.021

Cuillière, J.-C., François, V., Nana, A., 2018. Automatic construction of structural CAD models from 3D topology optimization. Comput.-Aided Des. Appl. 15, 107–121. https://doi.org/10.1080/16864360.2017.1353726

Dede, E., 2009. Multiphysics Topology Optimization of Heat Transfer and Fluid Flow Systems. Presented at the COMSOL Users Conference, Boston, USA.

Denk, M., Klemens, R., Paetzold, K., 2021a. Beam-colored Sketch and Image-based 3D Continuous Wireframe Reconstruction with different Materials and Cross-Sections, in: Stelzer, R., Krzywinski, J. (Eds.), Entwerfen Entwickeln Erleben in Produktentwicklung Und Design 2021. Presented at the Entwerfen Entwickeln Erleben, TUDpress, Dresden, pp. 345–354. https://doi.org/10.25368/2021.33

Denk, M., Rother, K., Paetzold, K., 2021b. Fully Automated Subdivision Surface Parametrization for Topology Optimized Structures and Frame Structures Using Euclidean Distance Transformation and Homotopic




https://doi.org/10.1017/pds.2022.38 Published online by Cambridge University Press

Thinning, in: Pfingstl, S., Horoschenkoff, A., Höfer, P., Zimmermann, M. (Eds.), Proceedings of the Munich Symposium on Lightweight Design 2020. Springer Berlin Heidelberg, Berlin, Heidelberg, pp. 18–27. https://doi.org/10.1007/978-3-662-63143-0_2
Denk, M., Rother, K., Paetzold, K., 2021c. Subdivision Surfaces Mid-Surface Reconstruction of Topology Optimization Results and Thin-Walled Shapes using Surface Seletons, in: Proceedings of the 21th International Conference on Engineering Design. Presented at the International Conference on Engineering Design (ICED21), Cambridge University Press, Goethenburg, pp. 2771–2780. https://doi.org/10.1017/pds.2021.538
Denk, M., Rother, K., Paetzold, K., 2020. Multi-Objective Topology Optimization of Heat Conduction and Linear Elastostatic using Weighted Global Criteria Method, in: Proceedings of the 31st Symposium Design for X (DFX2020), DFX. Presented at the DfX Symposium 2020, The Design Society, Bamberg, pp. 91–100. https://doi.org/10.35199/dfx2020.10
Denk, M., Rother, K., Zinßer, M., Petroll, C., Paetzold, K., 2021d. Nodal cosine sine material interpolation in multi objective topology optimization with the global criteria method for linear elasto static, heat transfer, potential flow and binary cross entropy sharpening., in: Proceedings of the 23th International Conference on Engineering Design. Presented at the International Conference on Engineering Design, Cambridge University Press, Götheburg, pp. 2247–2256. https://doi.org/10.1017/pds.2021.486
Gao, J., Luo, Z., Xiao, M., Gao, L., Li, P., 2020. A NURBS-based Multi-Material Interpolation (N-MMI) for isogeometric topology optimization of structures. Appl. Math. Model. 81, 818–843. https://doi.org/10.1016/j.apm.2020.01.006
Hitoshi, N., Makoto, H., Toshiyuki, K., Toru, K., Isao, S., Koichi, O., 1985. Object modeling by distribution function and a method of image generation. 電子通信学会論文誌 D 68, 718–725.
Hubert, E., Cani, M.-P., 2012. Convolution surfaces based on polygonal curve skeletons. J. Symb. Comput., Advances in Mathematics Mechanization 47, 680–699. https://doi.org/10.1016/j.jsc.2011.12.026
Joo, Y., Lee, I., Kim, S.J., 2018. Efficient three-dimensional topology optimization of heat sinks in natural convection using the shape-dependent convection model. Int. J. Heat Mass Transf. 127, 32–40. https://doi.org/10.1016/j.ijheatmasstransfer.2018.08.009
Karpenko, O., Hughes, J.F., Raskar, R., 2002. Free-form sketching with variational implicit surfaces. Comput. Graph. Forum 21, 585–594.
Lee, T.C., Kashyap, R.L., Chu, C.N., 1994. Building Skeleton Models via 3-D Medial Surface Axis Thinning Algorithms. CVGIP Graph. Models Image Process. 56, 462–478. https://doi.org/10.1006/cgip.1994.1042
Mayer, J., Wartzack, S., 2020. Ermittlung eines Skelettierungsverfahrens zur Konvertierung von Topologieoptimierungsergebnissen, in: Proceedings of the 31st Symposium Design for X (DFX2020). Presented at the Symposium Design for X 2020, Bamberg, pp. 111–120. https://doi.org/10.35199/dfx2020.12
Morgenthaler, D.G., 1981. Three-dimensional Simple Points: Serial Erosion, Parallel Thinning, and Skeletonization. University of Maryland.
Nana, A., Cuillière, J.-C., Francois, V., 2017. Automatic reconstruction of beam structures from 3D topology optimization results. Comput. Struct. 189, 62–82. https://doi.org/10.1016/j.compstruc.2017.04.018
Pan, J., Yan, S., Qin, H., 2016. Interactive Dissection of Digital Organs Based on Metaballs, in: Proceedings of the 33rd Computer Graphics International. Presented at the CGI '16: Computer Graphics International, ACM, Heraklion Greece, pp. 13–16. https://doi.org/10.1145/2949035.2949039
Sobiecki, A., Jalba, A., Telea, A., 2014. Comparison of curve and surface skeletonization methods for voxel shapes. Pattern Recognit. Lett. 47, 147–156. https://doi.org/10.1016/j.patrec.2014.01.012
Stangl, T., Wartzack, S., 2015. Feature based interpretation and reconstruction of structural topology optimization results, in: Weber, M., C.;. Husung, S.;. Cascini, G.;. Cantamessa, M.;. Marjanovic, D.;. Bordegoni (Ed.), Proceedings of the 20th International Conference on Engineering Design (ICED15). Design Society, p. Vol. 6, 235-245.
Tagliasacchi, A., Delame, T., Spagnuolo, M., Amenta, N., Telea, A., 2016. 3D Skeletons: A State-of-the-Art Report. Comput. Graph. Forum 35, 573–597. https://doi.org/10.1111/cgf.12865
Wyvill, G., McPheeters, C., Wyvill, B., 1986. Data structure for soft objects. Vis. Comput. 2, 227–234. https://doi.org/10.1007/BF01900346
Xia, Y., Langelaar, M., Hendriks, M., 2020. Optimization-based three-dimensional strut-and-tie model generation for reinforced concrete. Comput.-Aided Civ. Infrastruct. Eng. https://doi.org/10.1111/mice.12614
Xu, T.-C., Wu, E.-H., 2016. View-space meta-ball approximation by depth-independent accumulative fields, in: SIGGRAPH ASIA 2016 Technical Briefs, SA '16. Association for Computing Machinery, New York, NY, USA, pp. 1–4. https://doi.org/10.1145/3005358.3005389
Yin, G., Xiao, X., Cirak, F., 2020. Topologically robust CAD model generation for structural optimisation. Comput. Methods Appl. Mech. Eng. 369, 113102. https://doi.org/10.1016/j.cma.2020.113102